SAND98-2631 J

InGaAsN Solar Cells with 1.0 eV Bandgap, Lattice Matched to GaAs

Steven R. Kurtz, A. A. Allerman, E. D. Jones, J. M. Gee, J. J. Banas,

and B. E. Hammons

Sandia National Laboratories, Albuquerque, NM 87185-0603

The design, growth by metal-organic chemical vapor deposition, and processing of an $In_{0.07}Ga_{0.93}As_{0.98}N_{0.02}$ solar cell, with 1.0 eV bandgap, lattice matched to GaAs is described. The hole diffusion length in annealed, n-type InGaAsN is 0.6-0.8 μm, and solar cell internal quantum efficiencies > 70% are obtained. Optical studies indicate that defects or impurities, from InGaAsN doping and nitrogen incorporation, limit solar cell performance.

Multi-junction tandem solar cells are being developed as power sources for satellite systems operating in air mass zero (AM0) solar radiation. Models indicate that record efficiencies (≈ 38%) would be obtained for tandem cells where a 1.0 eV bandgap cell is added in series to proven InGaP-GaAs tandem structures.[1] The $In_xGa_{1-x}As_{1-y}N_y$ alloy system appears ideal for this application. Bandgaps of ≤ 1.0 eV are obtained for $In_xGa_{1-x}As_{1-y}N_y$ with minimal N concentrations ($y > 0.02$), and the quaternary is lattice-matched to GaAs for compositions with $x \approx 3y$. [2,3] Even at these low concentrations, N incorporation has proven problematic, and it remains a challenge to demonstrate thick (2-3 μm), high quality, $In_xGa_{1-x}As_{1-y}N_y$ ($y > 0.02$) epilayers needed for solar cell development. In this paper, we present a status report on $In_xGa_{1-x}As_{1-y}N_y$ properties, growth, and solar cell performance. Under specialized conditions, we demonstrate internal quantum efficiencies >70 % for 1.0 eV bandgap solar cells.

The structures in this work were grown in a vertical flow, high speed rotating disk, Emcore GS/3200 metalorganic chemical vapor deposition (MOCVD) reactor. $In_xGa_{1-x}As_{1-y}N_y$ films were grown using trimethylindium (TMIn), trimethylgallium (TMG), 100% arsine and dimethylhydrazine (DMHy). Dimethylhydrazine was used as the nitrogen source since it has a lower disassociation temperature than ammonia and has a vapor pressure of approximately 110 torr at 18°C. Unintentionally doped InGaAsN was p-type. N-type material was achieved using silicon tetrachloride ($SiCl_4$). InGaAsN films for Hall and optical measurements were grown on semi-insulating GaAs orientated 2° off (100) towards <110>. Lattice matched ($\Delta a/a < 8 \times 10^{-4}$) films were grown at 600 °C and 60 torr using a V/III ratio of 97, a DMHy/V ratio of 0.97 and a TMIn/V ratio of 0.12 . The growth rate was 10Å/s. These conditions resulted in films with an indium mole

DISCLAIMER

fraction of 0.07 (±0.005) and a nitrogen mole fraction of 0.022 (±0.003). The composition was determined by calibration growths of GaAsN and InGaAs along with double crystal x-ray diffraction measurements. The nitrogen composition was also confirmed from elastic recoil detection (ERD) measurements.

A significant increase in photoluminescence intensity was observed from these films following a post-growth anneal.[4] Ex-situ, post –growth anneals were carried out in a rapid thermal anneal system under nitrogen using a sacrificial GaAs wafer in close proximity to the InGaAsN sample. The photoluminescence intensity was a maximum for samples annealed for either 700°C for 2 minutes or 650°C for 30 minutes. Secondary ion mass spectrometry measurements showed the residual carbon concentration of similar films to be 6-8x10^{17} cm^{-3}. Carbon is incorporated during growth at sufficiently high levels to possibly cause the background p-type conductivity and the observed ex-situ annealing behavior.

The optical properties of the InGaAsN films were extremely sensitive to N content, ex-situ annealing, and doping. Photoluminescence and optical absorption spectra are shown in Figure 1 for InGaAsN films grown under the same conditions and with nominally the same compositions as the n and p-type regions of the solar cell. Photoluminescence was measured with a Fourier transform spectrometer equipped with a cooled, North Coast Ge detector. In addition to the bandgap reduction, there was photoluminescence quenching in InGaAsN films with increasing N content. A band-edge photoluminescence peak was not observed in as-grown, $In_{0.07}Ga_{0.93}As_{0.98}N_{0.02}$ films at 300 K. After the ex-situ annealing process, described earlier, a band-edge photoluminescence peak, approximately 60 meV linewidth, was observed in our p-type

films. (see Figure 1(a)) Annealing had negligible affect on the absorption spectra of the p-type films. (Absorption spectra are shown in Fig. 1(b). Baseline corrections have eliminated free carrier contributions to these spectra .) Consistent with these observations, deep-level-transient-spectroscopy (DLTS) results clearly show that annealing eliminates a midgap defect state present in our as-grown, p-type material.[5] N-type doping with Si appears to introduce yet another defect or impurity into the InGaAsN. With Si doping, the band-edge photoluminescence was weak both before and after ex-situ annealing. (Fig. 1(a)) Also, the absorption spectrum for the Si doped material displayed a low energy tail. (Fig. 1(b)) DLTS measurements to identify the defect associated with Si doping are in progress.[7]

The solar cell described in this work consisted of a 1.0 μm thick, n-type (2×10^{17} cm^{-3}, Si doped) $In_{0.07}Ga_{0.93}As_{0.98}N_{0.02}$ emitter grown on a 1.0 μm thick, p-type (4×10^{16} cm^{-3}, background doped) base. The base doping concentration was determined from capacitance-voltage measurements, and emitter doping was determined from Hall measurements on similar, annealed material. The solar cell was grown on a p+ GaAs substrate. A 500 Å thick, $Al_{0.8}Ga_{0.2}As$ window layer and a 0.15 μm thick GaAs cap/contact layer (both doped n-type, $5x10^{18}/cm^3$) were grown on top of the solar cell emitter. The $Al_{0.8}Ga_{0.2}As$ window prevented photogenerated holes from escaping from the n-type emitter, and the 300-400 meV $In_{0.07}Ga_{0.93}As_{0.98}N_{0.02}$ / GaAs conduction band offset produced a back-side reflector for electrons generated in the p-type base. Solar cells were processed with Pd/Ge/Au front grids and Be/Au back contacts and with an area of 0.25 cm^2. Any ex-situ anneals of InGaAsN were performed prior to metallization. No antireflection coatings were applied.

Solar cell spectral response was determined by the ratio of the short-circuit cell photocurrent to that of a calibrated Ge detector. The internal quantum efficiency curves for both the annealed and as-grown cells are shown in Figure 2. The photoresponses extended out to the band-edge of the InGaAsN at 1.2 μm. (Due to irreproducibility in N composition, the solar cell bandgap was shifted to ≈ 0.04 μm longer wavelength than that of the optical samples shown in Fig.1) At wavelengths less than 0.9 μm, the solar cell response was dominated by the GaAs cap, acting as a filter. Peak internal quantum efficiencies of >70% were obtained for the annealed cell. Comparing the annealed and as-grown cells, annealing improved the quantum efficiency by roughly a factor of 5. Comparing the performance of our thick n-type emitter solar cell with thin n-type emitter cells and other alternative designs, we found that negligible electron diffusion is occurring in the 1.0 eV p-type material (annealed or as-grown). To date, high quantum efficiencies have only been obtained with cell designs utilizing hole diffusion in n-type material.

Previously, InGaAsN solar cells have displayed short minority carrier diffusion lengths, and their photocurrents have been dominated by electron-hole pairs generated in the depletion region. The highest internal quantum efficiency reported for an InGaAsN solar cell was ≥ 60% (@ 1.1 μm), achieved with a compensation-doped p-i-n device . Conventional p-n InGaAsN solar cells have displayed internal quantum efficiencies typically < 25 % (@1.1 μm).[7] To estimate the minority carrier diffusion length in our cells, we measured the photocurrent response versus bias. Depletion widths were determined from capacitance-voltage measurements. As shown in Figure 3, the photocurrents of the annealed and as-grown cells displayed roughly the same dependence

on depletion width, although the photocurrent was much larger for the annealed cell. Based on several diagnostic devices, we developed a model which included carrier collection from the n-type emitter and the depletion region. From the model, one finds $\alpha L \approx 1.1$ and 0.35 for the annealed and as-grown samples, respectively, where α is the absorption coefficient and L is the minority carrier diffusion length. From absorption data, we estimate that the hole diffusion lengths are 0.6-0.8 μm (annealed) and 0.2-0.3 μm (as-grown). Despite the poor quality of the n-type material as indicated by optical studies, the improved efficiency of our annealed InGaAsN cell was due to diffusion of holes in the n-type emitter.

Solar cell current-voltage characteristics were measured under high flux, broadband illumination conditions. For various light intensities, open-circuit voltage (V_{oc}) and short-circuit current (I_{sc}) values for the annealed and as-grown cells are shown in Figure 4. Annealing decreased the saturation current (I_0) from 1.1×10^{-6} A/cm^2 (as-grown) to 8.3×10^{-7} A/cm^2 (annealed). Similarly, the diode ideality factor (n) approached unity with annealing. (n=1.21 annealed versus n=1.33 as-grown) For the solar cell shown, the open circuit voltage was low ($\leq$ 0.3 V). As bandgap energy increases, we found that the open circuit voltage rapidly increased. For example, the open-circuit voltage of a high efficiency, 1.2 eV bandgap InGaAsN solar cell was 0.6 V for I_{sc}=0.03 A/cm^2 ($I_0=1.1 \times 10^{-11}$ A/cm^2). Hopefully, we will be able to demonstrate future improvements in minority carrier diffusion length and lifetime to approach the open-circuit voltages (0.6-0.7 V) which are theoretically predicted for 1.0 eV bandgap InGaAsN solar cells.

In summary, we have described the design, MOCVD growth, and processing of an InGaAsN solar cell with improved performance. Unlike previous cells, we have demonstrated viable minority carrier diffusion, and in our present devices, we realized >70% internal quantum efficiency. The hole diffusion length in annealed, n-type 1.0 eV bandgap InGaAsN was 0.6-0.8 μm, and we found that ex-situ annealing was required to turn-on the hole diffusion. Even with future realization of near-unity quantum efficiency, material-related improvements in minority carrier lifetime and diffusion length will be required to increase 1.0 eV bandgap InGaAsN cell open-circuit voltages from ≈ 0.3 V. Optical studies indicated that there are defects present in the InGaAsN associated with both N incorporation and n-type, Si doping. Elimination of such defects should further improve the performance of InGaAsN solar cells.

The authors thank J. A. Bur and M. J. Russell for technical support and H. Q. Hou, I. J. Fritz, J. F. Klem, and C. H. Seager for discussions and contributions to the InGaAsN project. A. Clement-font and J. Banks provided the ERD results. Sandia is a multiprogram laboratory operated by Sandia Corporation, a Lockheed Martin Company, for the U.S. Dept. of Energy under contract DE-AC04-94AL85000. Additional funding was provided by Air Force Weapons Laboratory.

References:

1. Sarah R. Kurtz, D. Myers, and J. M. Olsen, Proc. 26th IEEE Photovoltaics Spec. Conf., 875 (1997).

2. M. Weyers, M. Sato, and H. Ando, Jpn. J. Appl Phys. 31, 853 (1992).

3. S. Sato, Y. Osawa, and T. Saitoh, Jpn. J. Appl. Phys. 36, 2671 (1997).

4. E. V. K. Rao, A. Ougazzaden, Y. Le Bellego, and M. Juhel, Appl . Phys. Lett. 72, 1409 (1998).

5. C. H. Seager, Steven R. Kurtz, and A. A. Allerman, (unpublished).

6. S. A. Ringle (private communication).

7. D. J. Friedman, J. F. Geiz, Sarah R. Kurtz, and J. M. Olsen, Proc. of 2nd World Conf. on Photovoltaic Energy Conv., 1998 (in press).

Figure Captions:

Figure 1 – (a) Photoluminescence spectra for ex-situ annealed, p-type (background doped) and n-type (Si doped) $In_{0.07}Ga_{0.93}As_{0.98}N_{0.02}$ epitaxial films. (b) Absorption spectra for the samples in (a).

Figure 2 – Internal quantum efficiency curves for as-grown (0V bias, 0.15 μm depletion width) and ex-situ annealed (0V bias, 0.26 μm depletion width) $In_{0.07}Ga_{0.93}As_{0.98}N_{0.02}$ solar cells with 1.0 μm thick, n-type emitters.

Figure 3 – Internal quantum efficiency versus depletion width for the as-grown and annealed solar cells. Model (solid lines) assumes that the ratio of the n and p-type doping concentrations is unchanged by annealing.

Figure 4 – Measured solar cell open-circuit voltage (V_{OC}) and short-circuit current (I_{SC}) for various light intensities.

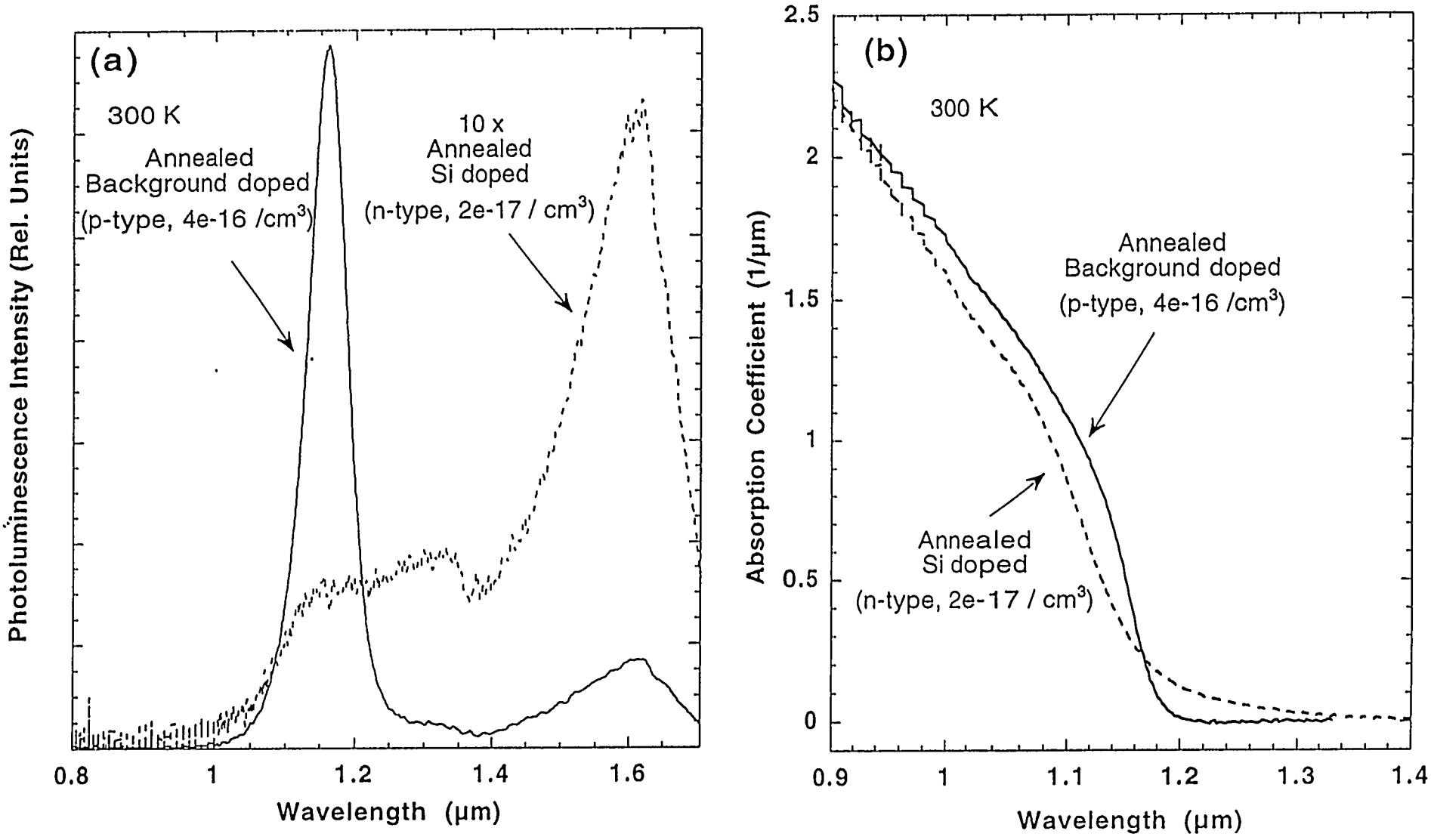
(a)
300 K
Annealed
Background doped
(p-type, 4e-16 /cm3)
10 x
Annealed
Si doped
(n-type, 2e-17 / cm3)
Photoluminescence Intensity (Rel. Units)
0.8
1
1.2
1.4
1.6
Wavelength (μm)
(b)
300 K
Annealed
Background doped
(p-type, 4e-16 /cm3)
Annealed
Si doped
(n-type, 2e-17 / cm3)
Absorption Coefficient (1/μm)
2.5
2
1.5
1
0.5
0
0.9
1
1.1
1.2
1.3
1.4
Wavelength (μm)

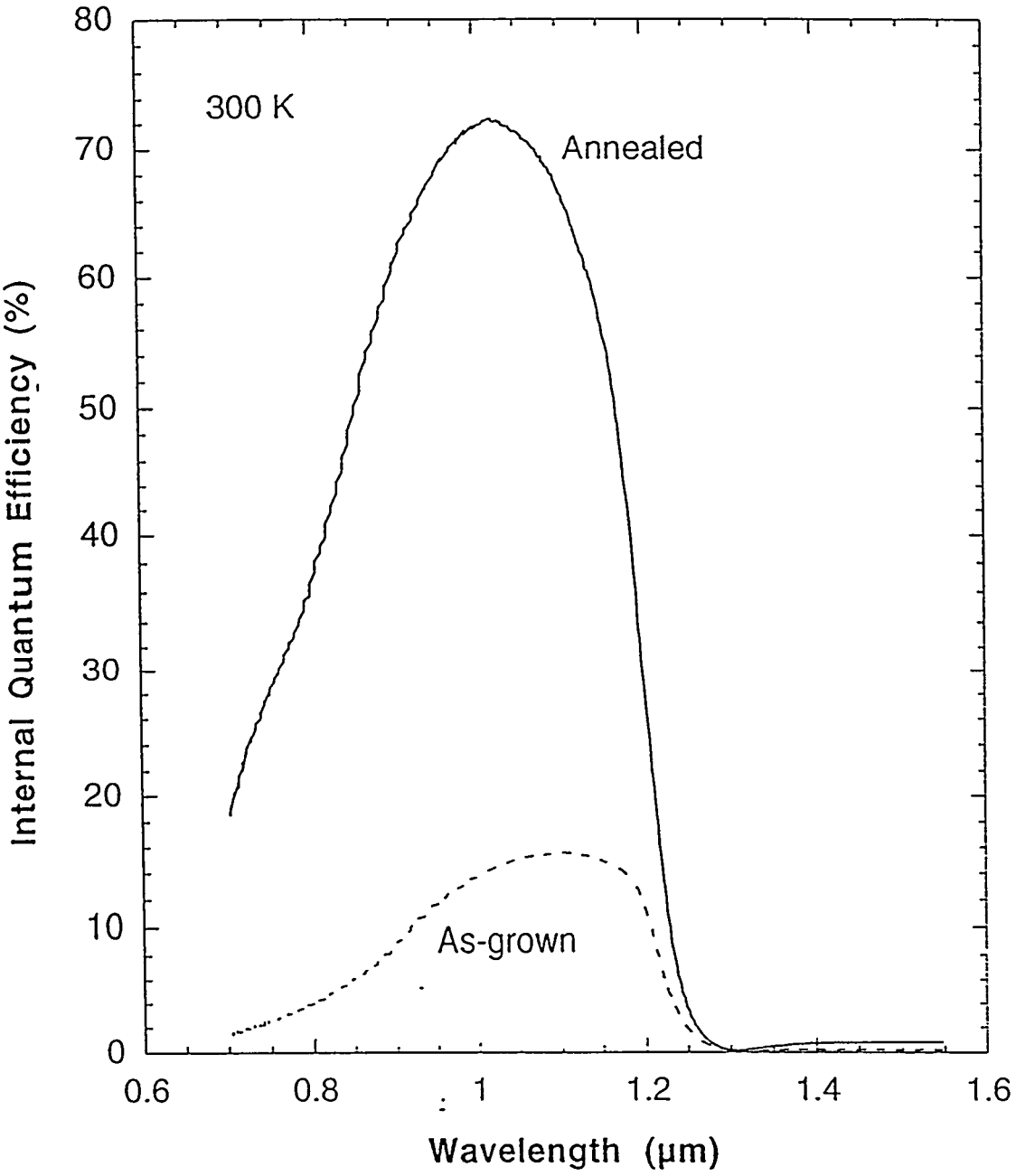
300 K
Annealed
As-grown
Internal Quantum Efficiency (%)
Wavelength (μm)
0
10
20
30
40
50
60
70
80
0.6
0.8
1
1.2
1.4
1.6

Fig. 2

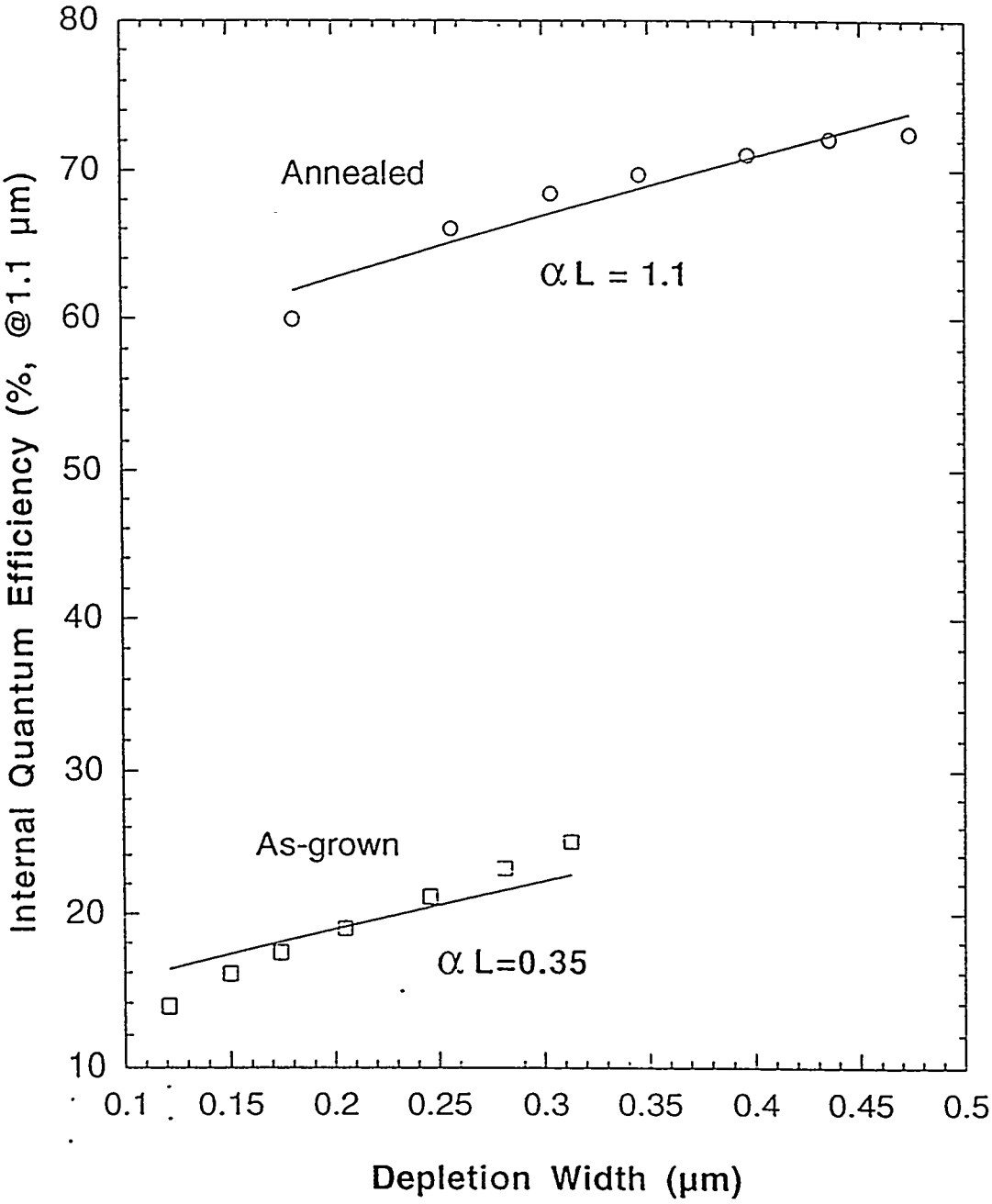
Internal Quantum Efficiency (%, @1.1 μm)
80
70
60
50
40
30
20
10
0.1
0.15
0.2
0.25
0.3
0.35
0.4
0.45
0.5
Depletion Width (μm)
Annealed
αL = 1.1
As-grown
αL=0.35

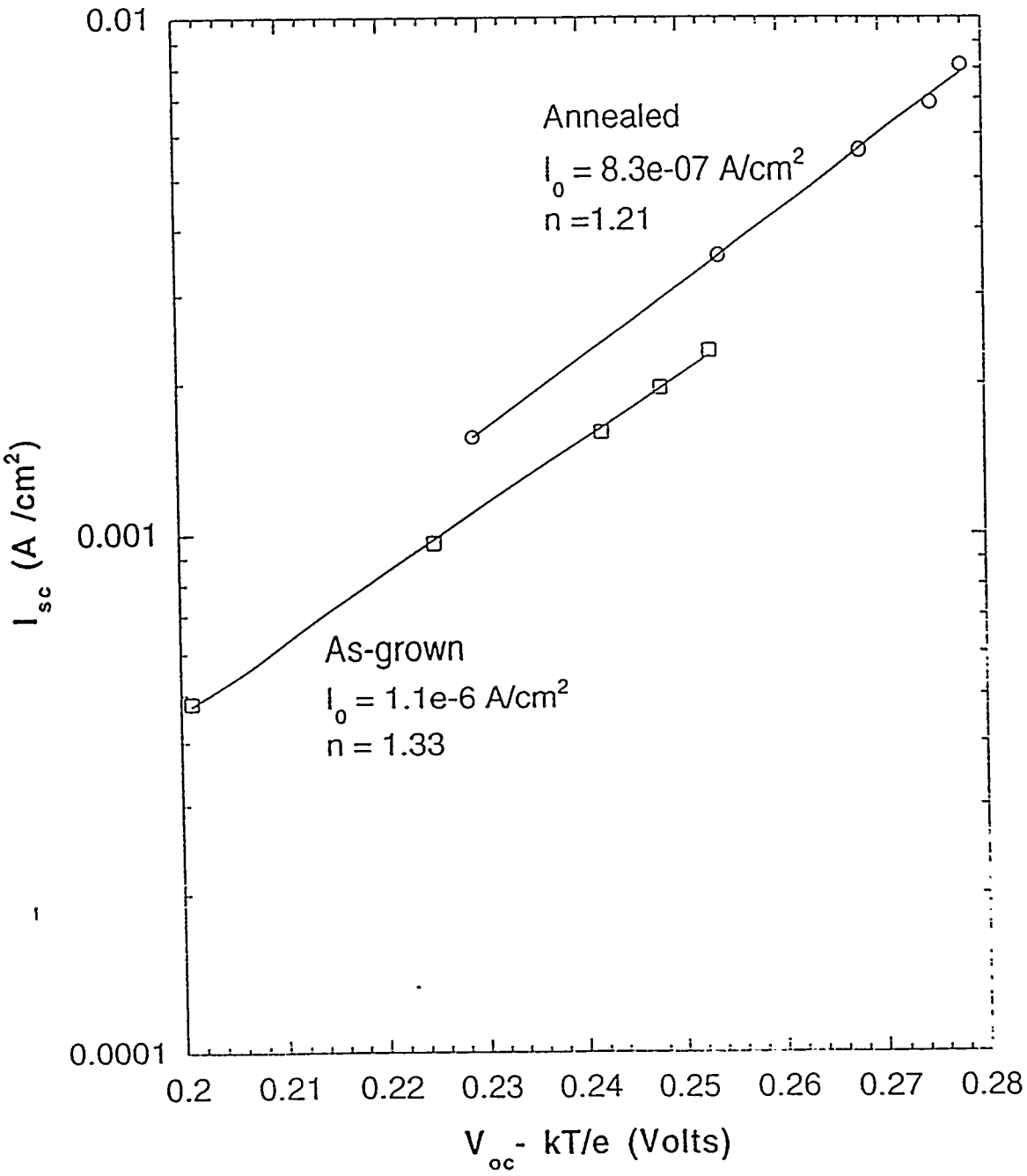
0.01
0.001
0.0001
I_{sc} (A /cm^2)
Annealed
I_0 = 8.3e-07 A/cm^2
n =1.21
As-grown
I_0 = 1.1e-6 A/cm^2
n = 1.33
0.2
0.21
0.22
0.23
0.24
0.25
0.26
0.27
0.28
V_{oc} - kT/e (Volts)